US National Oceanic and Atmospheric Administration
Climate Test Bed Joint Seminar Series
NCEP, Camp Springs, Maryland, 3 February 2010

ENSO Prediction Skill in the NCEP CFS

Renguang Wu[1], Ben P. Kirtman[1,2] and Huug van den Dool[3]

[1]*Center for Ocean-Land-Atmosphere Studies, Calverton, Maryland*
[2]*Rosenstiel School of Marine and Atmospheric Science, University of Miami, Miami, FL*
[3]*Climate Prediction Center, National Centers for Environmental Prediction, Camp Springs, MD*

1. Introduction

A well-known feature in ENSO forecasts is a significant drop in prediction skill during boreal spring (Kirtman *et al.* 2001), particularly in terms of eastern Pacific SST correlation coefficients. This spring prediction barrier has been attributed to the low variance of NINO3 SST anomalies in boreal spring (Xue *et al.* 1994; Torrence and Webster 1998; Clarke and Van Gorder 1999). In the spring season, the Walker circulation is weak and the east-west sea level pressure and SST gradient along the equatorial Pacific is at a minimum (Webster and Yang 1992; Webster 1995; Lau and Yang 1996). Under such conditions, the initial errors and "weather" noise in the models can project strongly onto ENSO modes, leading to large error growth and deteriorating the forecasts. Chen *et al.* (1995) suggested that the spring predictability barrier is not intrinsic to the real climate system and that it may be a problem of the models. Jin and Kinter (2009) indicated that systematic model errors are major factors limiting the predictability and degrading the forecast skill.

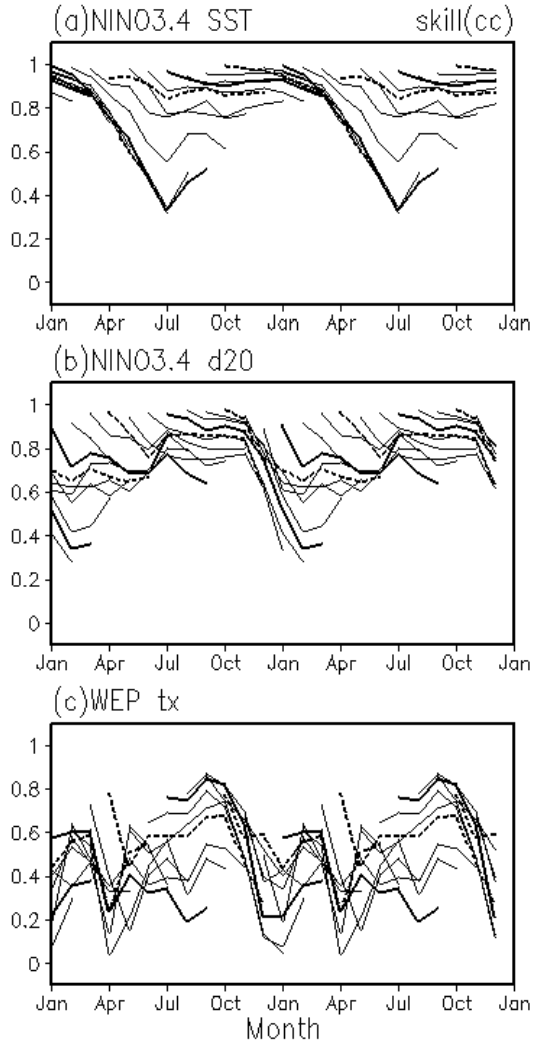

Fig. 1 Correlation skill of NINO3.4 SST (a), NINO3.4 thermocline depth (b), and western equatorial Pacific zonal wind stress (c) derived from CFS ensemble mean forecasts. For clarity of presentation two repeating years are shown.

One important factor for the eastern equatorial SST anomalies is the equatorial Pacific thermocline change. Thus, it may be asked whether there is a similar prediction barrier in the thermocline. Indeed, a boreal winter prediction barrier was identified in the equatorial Pacific heat content (Balmaseda *et al.* 1995). In analogy with low NINO3 SST variance in boreal spring, the equatorial Pacific warm water volume anomalies tend to have small variance in boreal winter (McPhaden 2003). Since equatorial Pacific heat content fluctuations are closely related to surface wind changes in the western equatorial Pacific (Kirtman 1997; Weisberg and Wang 1997; Mayer and Weisberg 1998; Wang *et al.* 1999), is there an associated barrier for the low level winds in that area?

The NCEP CFS (Saha *et al.* 2006) has become an important forecast tool. Because of the large impacts of ENSO on climate fluctuations in both the tropics and extratropics, it is important to understand how the CFS performs in terms of tropical Pacific SST forecasts. Saha et al. (2006) have shown that the CFS SST forecasts experience a large drop in skill in boreal spring. What are the plausible reasons for the drop in skill? Is it due to the effects of noise or related to the reduction of signal-to-noise ratio (Torrence and Webster 1998)?

Correspondence to: Renguang Wu, Center for Ocean-Land-Atmosphere Studies, 4041 Powder Mill Road, Suite 302, Calverton, MD 20705; E-mail: renguang@cola.iges.org

Understanding these questions would help toward a better application of ENSO forecasts made based on the CFS. The present study addresses these questions based on the NCEP CFS 24-year retrospective ensemble forecasts.

2. The prediction barrier

Here, the prediction skill is measured by the correlation coefficient between the CFS ensemble mean forecasts and observations. The prediction skill is calculated based on area-mean anomalies. Figure 1 shows the prediction skills for the NINO3.4 (5°S-5°N, 170°-120°W) SST, NINO3.4 thermocline depth, and the western equatorial Pacific (5°S-5°N, 130°-170°E) zonal wind stress.

The NINO3.4 SST forecast skill has an apparent drop during April-June for forecasts starting before March (Fig. 1a). The lowest forecast skill (less than 0.4) appears in July for forecasts starting from November-January. For forecasts starting after March, the drop in skill is much less with correlations maintained at a high level during November-February. These results are consistent with Saha *et al.* (2006), and with reported skill by many other methods as well (see Kirtman *et al.* 2001).

The NINO3.4 thermocline depth experiences an obvious drop in the forecast skill as well. The deterioration of skill is seen during December-February with the lowest forecast skill appearing in February-March (Fig. 1b), leading the drop in skill in the NINO3.4 SST by about 4-5 months. The time difference of the drop in skill between the NINO3.4 SST and thermocline depth is consistent with their phase lag as shown in previous studies (Zebiak and Cane 1987; Balmaseda *et al.* 1995). This suggests that the changes in the forecast skill for these two quantities are related.

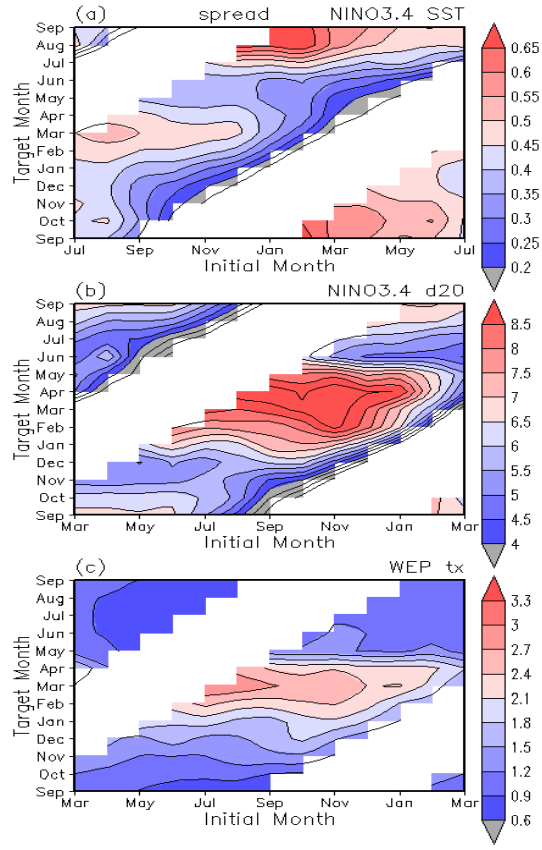

Fig. 2 Ensemble spread for monthly mean NINO3.4 SST (a), NINO3.4 thermocline depth (b), and western equatorial Pacific zonal wind stress (c) derived from CFS forecasts.

The western equatorial Pacific zonal wind stress shows generally lower skill compared to the NINO3.4 SST and thermocline depth. There are three periods during which the forecast skill for the wind stress displays obvious drops. The first and most pronounced one is during October-December (Fig. 1c). This one leads the drop in skill in the NINO3.4 thermocline depth by about 1-2 months. In view of the phase relationship between the western equatorial Pacific wind stress and equatorial Pacific thermocline changes in the ENSO evolution (Wang *et al.* 1999), this drop in skill in the wind stress is likely related to that in the thermocline depth. The second drop in skill is seen in March-April, which is likely related to the effects of atmospheric noise. Another drop in skill is seen in July-August. Compared to the other two, this latter drop in skill is relatively weak and is only seen for some of the forecasts.

Previous studies have focused on the substantial decrease in observation-prediction correlation in the NINO3 SST or the SO index across the boreal spring and have attributed the spring prediction barrier to the maximum error growth in boreal spring (*e.g.*, Webster 1995). The forecast skill in Fig. 1 shows that the drop in skill in NINO3.4 thermocline depth and western equatorial Pacific surface wind stress precedes the drop in skill in NINO3.4 SST in boreal spring. This phase relationship suggests that the prediction barrier could be an intrinsic feature of the coupled model (i.e., coupled model error), although the noise may also play a role.

3. Possible reasons for the prediction barrier

If the noise is critical to the low skill, then we would expect to see large noise when the skill drops. To examine, whether this is so, we show in Fig. 2 the ensemble spread for the NINO3.4 SST, NINO3.4

thermocline depth, and the western equatorial Pacific zonal wind stress. Here, the ensemble spread is used as a proxy for noise.

For the NINO3.4 SST, the largest spread is seen around August-September (Fig. 2a) when the eastern equatorial Pacific cold tongue is the coldest and the SST front surrounding the cold tongue is the strongest. The spread is small around May when the skill drops quickly. For the NINO3.4 thermocline depth, the largest spread is seen around March-April for most of the forecasts (Fig. 2b). Around December when the skill drop, the spread is small. For the western equatorial Pacific zonal wind stress, the largest spread is around March (Fig. 2c), which coincides with the secondary skill drop. The main skill drop around November is in a period when the spread increases. The temporal relationship between the seasonal change of the prediction skill and the spread indicates that the prediction barrier is unlikely to be explained by the noise variation.

To further demonstrate whether the noise contributes to the drop in the prediction skill, we show in Fig. 3 the correlation skill of three quantities calculated using the "perfect model approach" based on the 15-member forecasts. In this calculation, one member of the forecasts is treated as "observation" and the ensemble mean of the other 14 members is treated as "forecast". The correlation is calculated for each of the 15 members alternatively treated as "observation" and Fig. 3 shows the mean of the 15 correlations calculated for NINO3.4 SST, NINO3.4 thermocline depth, and the western equatorial Pacific zonal wind stress. Under the perfect model assumption, the model systematic errors do not exist and thus the change in the correlation skill is attributed to the impacts of noise and initial condition errors. Comparison of Fig. 3 and Fig. 1 illustrates whether noise contributes to the prediction skill and to what extent.

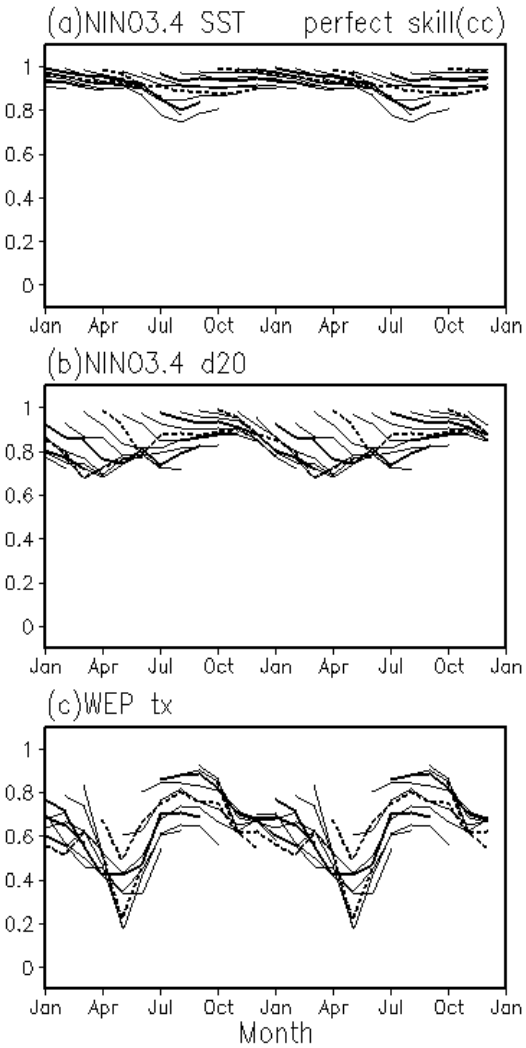

Fig. 3 Correlation skill of NINO3.4 SST (a), NINO3.4 thermocline depth (b), and western equatorial Pacific zonal wind stress (c) calculated using the perfect model approach from CFS forecasts.

For NINO3.4 SST, the lowest predictability is seen during July-September (Fig. 3a), consistent with Saha *et al.* (2006, their Fig.3). The drop in skill, however, is only about 0.2, much less than that seen in Fig. 1a. In addition, the timing of the drop in skill is later than that seen in Fig. 1a. For NINO3.4 thermocline depth, the drop in skill is larger compared to NINO3.4 SST. The lowest skill is about 0.7 during March-April (Fig. 3b). The low skill in the thermocline depth leads that in the SST by about 4-5 months. For some of the forecasts, there is a secondary correlation minimum in July. Compared to the skill in Fig. 1b, the drop in skill is much less and occurs at a later time. For the western equatorial Pacific zonal wind stress, the drop in skill is more pronounced, with the lowest correlations occurring around May (Fig. 3c). The drop in skill during March-April seems to occur at the same time as the one of the drops seen in Fig 1c.

The above relationship indicates that the noise does not entirely explain the drops in the prediction skill seen in the CFS ensemble forecasts. The question then is, what is responsible for the decline in the prediction skill? Our analyses suggest that the CFS atmospheric wind response to SST anomalies is significantly different from observations, and that this difference is amplified by coupled feedback, ultimately leading to the spring prediction barrier. This is demonstrated in the following.

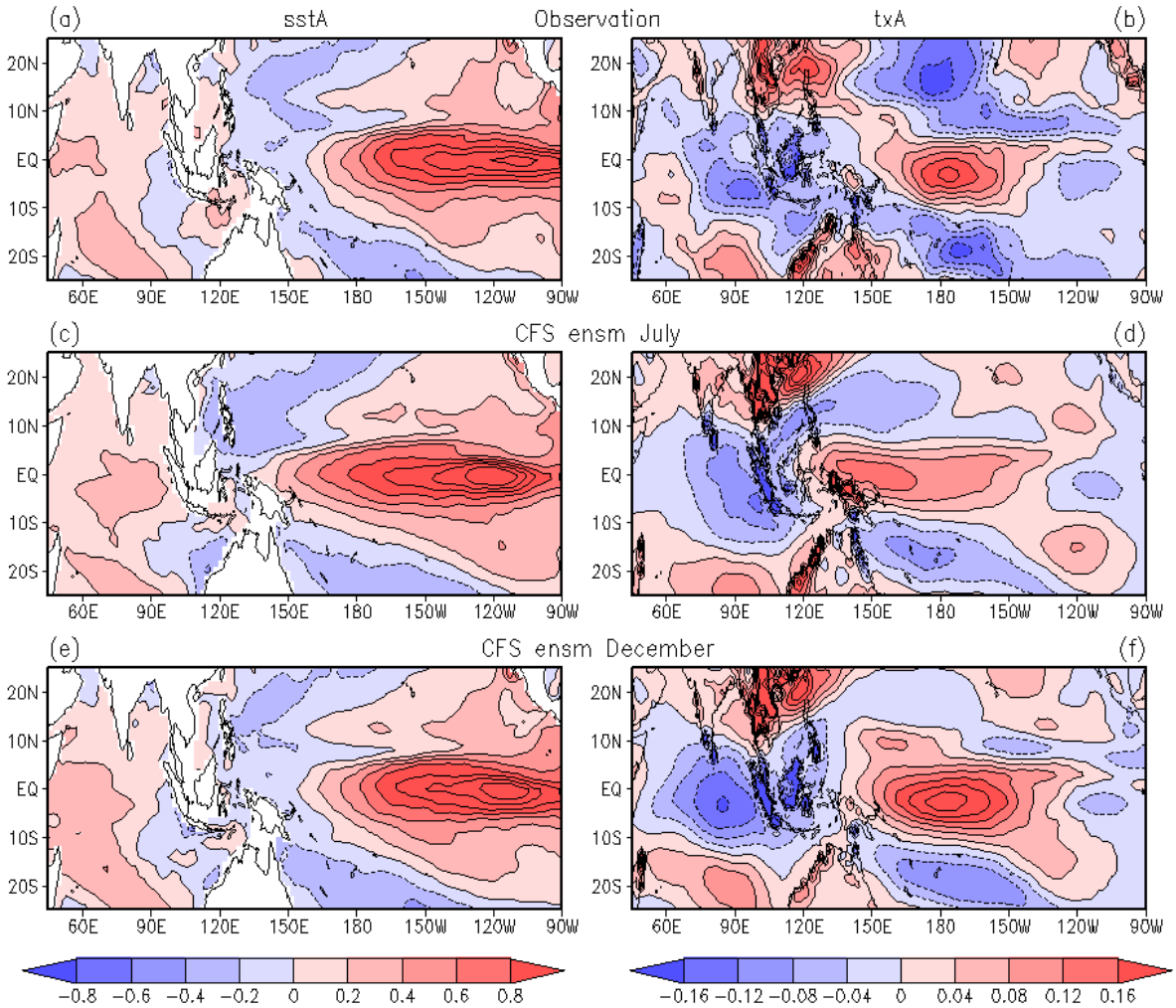

Fig. 4 Anomalies of December SST (°C) (a, c, e) and zonal wind stress (dyn/cm^2) (b, d, f) obtained as regression on December NINO3.4 SST. (a)-(b) are derived from observations, (c)-(d) from CFS ensemble mean forecasts starting from July, (e)-(f) from CFS ensemble mean forecasts starting from December. The contour interval is 0.2°C for SST and 0.04 dyn/cm^2 for wind stress.

Figure 4 shows the December SST and surface zonal wind stress anomalies obtained by regression onto the December NINO3.4 SST for observations, the CFS forecasts from July and December. For the forecasts initialized in December, the SST anomalies in the tropical Indo-Pacific Ocean (Fig. 4e) are in good agreement with the observational estimates (Fig. 4a). The zonal wind stress, however, shows noticeable differences. The anomalous westerly winds over the equatorial central Pacific are larger in the CFS forecasts (Fig. 4f) than in observations (Fig. 4b). In addition, the westerly winds extend more westward in the forecasts compared to observations. For the forecasts starting from July, the westward extension of anomalous westerly winds is more obvious (Fig. 4d). This is accompanied by westward extension of positive SST anomalies (Fig. 4c).

The differences in the zonal wind stress can affect the ENSO phase transition through ocean-atmosphere coupled processes. Figure 5 shows the temporal evolution of NINO3.4 SST, NINO3.4 thermocline depth, NINO3.4 zonal wind stress, and western equatorial Pacific zonal wind stress from CFS forecasts starting from December and July and from observations, which are obtained by regression onto December NINO3.4 SST. For forecasts starting from December, the initial month (December) NINO3.4 SST anomalies are nearly the same in the forecasts and observations (Fig. 5a). The westerly wind stress anomalies, however, are very different. Compared to observations, anomalous westerlies in the NINO3.4 region are larger throughout the 9-month forecast period (Fig. 5d) and those in the western equatorial Pacific are larger in December (Fig. 5c).

The larger westerly anomalies favor the maintaining of positive thermocline depth anomalies in the NINO3.4 region for a longer period in the CFS forecasts than in observations (Fig. 5b). This leads to a longer persistence of positive SST anomalies in the NINO3.4 region (Fig. 5a) and, in turn, to westerly anomalies over the equatorial central Pacific (Fig. 5d). At the time when observed SST anomalies are near zero, the CFS forecasts still have about 0.5°C positive SST anomalies. As such, low correlation skill appears at the time of observed phase transition. Note that, in March and April, the CFS forecast western equatorial Pacific wind anomalies are easterly (Fig. 5c), which cannot be explained by SST anomalies in the central-eastern equatorial Pacific. This suggests the impacts of other factors.

The differences in the time of phase transition of western equatorial Pacific zonal wind stress and NINO3.4 thermocline depth anomalies are more clearly seen in the forecasts starting from July. For these forecasts, westerly wind anomalies in the western equatorial Pacific are large and remain so until February, whereas in observations the westerly anomalies start to decrease quickly around November and become small in February (Fig. 5g). The differences in the NINO3.4 zonal wind stress anomalies are small before December, but after that these anomalies are larger in the forecasts than in observations (Fig. 5h). Corresponding to these wind stress differences, the CFS forecasts maintain positive thermocline depth anomalies in the NINO3.4 region for a longer time, whereas in observations the thermocline depth anomalies become small after December (Fig. 5f). This seems to delay the weakening of positive SST anomalies in the NINO3.4 region in the forecasts compared to observations (Fig. 5e). The differences in SST anomalies, in turn, contribute to larger westerly anomalies, in particular, during December-February (Figs. 5g-h).

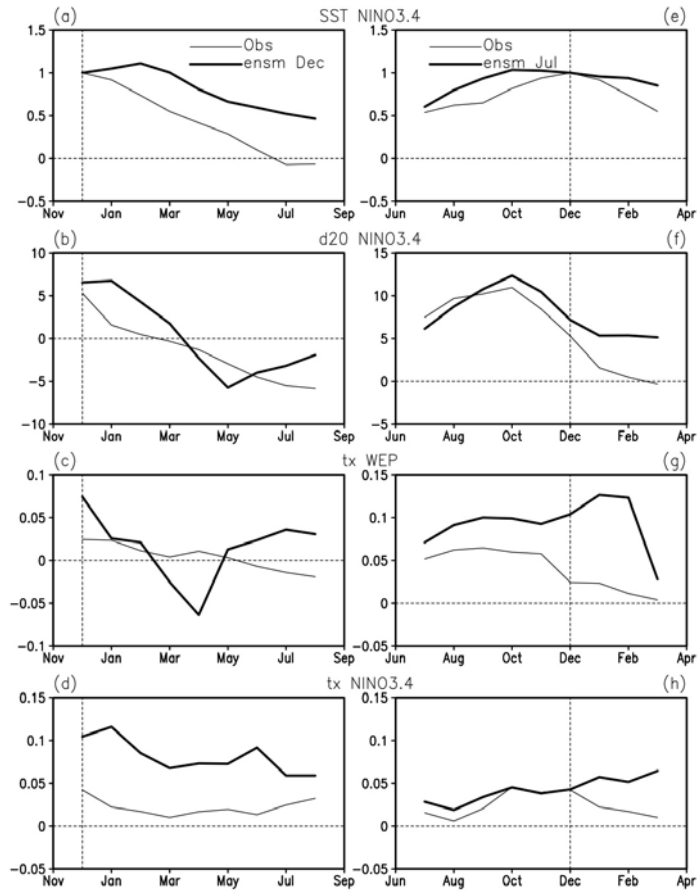

Fig. 5 Anomalies of NINO3.4 SST (°C) (a, e), NINO3.4 thermocline depth (m) (b, d), western equatorial Pacific zonal wind stress (dyn/cm^2) (c, g), and NINO3.4 zonal wind stress (dyn/cm^2) (d, h) obtained as regression on December NINO3.4 SST. (a)-(d) are from observations and CFS ensemble mean forecasts starting from December, (e)-(h) are the from observations and CFS ensemble mean forecasts starting from July. Thin curves are for observations and thick curves are for CFS ensemble mean forecasts.

4. Summary

The SST, thermocline depth, and surface wind stress over the equatorial Pacific are closely coupled. Model forecasts of ENSO have often encountered a reduced skill in boreal spring. The present study shows that the CFS retrospective forecasts experience a prominent drop in skill in boreal spring for NINO3.4 SST forecasts, in agreement with Saha *et al.* (2006), and this is preceded by a drop in skill in boreal winter in the NINO3.4 thermocline depth and western equatorial Pacific zonal wind stress.

The atmospheric noise has a large impact on the prediction skill of the zonal wind stress in boreal spring. However, its effects on the prediction skill in association with ENSO are relatively small with this model. The analysis presented here shows that in the CFS the atmospheric wind response to ENSO-related SST anomalies

is too strong and extends too westward. This deficiency seems to be amplified by coupled processes. As a result, the thermocline depth anomalies actually persist for too long and the ENSO phase transition is delayed in the CFS compared to observations. Our interpretation of this result is that the excessive persistence or delayed phase transition associated with wind stress structural errors is why CFS has a spring prediction barrier. Our results suggest that the spring prediction barrier is largely due to deficiencies in the models, in agreement with Chen *et al.* (1995) and Jin and Kinter (2009).

Previous studies have shown that the western equatorial Pacific zonal wind stress is an important element in the ENSO evolution (*e.g.*, Weisberg and Wang 1997; Wang *et al.* 1999). Not surprisingly, the present study indicates that the ENSO prediction skill is closely linked to the wind stress prediction skill. However, we also suggest that by improving the atmospheric model wind stress response to SST anomalies we can expect an improvement in ENSO forecast skill.

References

Balmaseda, M. A., M. K. Davey, and D. L. T. Anderson, 1995: Decadal and seasonal dependence of ENSO prediction skill. *J. Climate*, **8**, 2705-2715,

Chen, D., S. E. Zebiak, A. J. Busalacchi, and M. A. Cane, 1995: An improved procedure for El Niño forecasting. *Science*, **269**, 1699-1702.

Clarke, A. J., and S. Van Gorder, 1999: The connection between the boreal spring Southern Oscillation persistence barrier and biennial variability. *J. Climate*, **12**, 612-620.

Jin, E. K., and J. L. Kinter III, 2009: Characteristics of tropical Pacific SST predictability in coupled GCM forecasts using the NCEP CFS. *Clim. Dyn.*, 32, 675-691.

Kirtman, B. P., 1997: Oceanic Rossby wave dynamics and the ENSO period in a coupled model. *J. Climate*, **10**, 1690-1705.

Kirtman, B. P., J. Shukla, M. A. Balmaseda, N. E. Graham, C. Penland, Y. Xue, and S. E. Zebiak, 2001: Current status of ENSO forecast skill: A report to the Climate Variability and Predictability (CLIVAR) Numerical Experimentation Group (NEG), WCRP Informal Report No. 23/01, 31pp. [Available at http://www.clivar.org/publications/wg_reports/wgsip/nino3/report.htm]

Lau, K.-M., and S. Yang, 1996: The Asian monsoon and predictability of the tropical ocean-atmosphere system. *Quart. J. Roy. Meteorol. Soc.*, **122**, 945-957.

Mayer, D. A., and R. H. Weisberg, 1998: El Niño-Southern Oscillation-related ocean-atmosphere coupling in the western equatorial Pacific. *J. Geophys. Res.*, **103(C9)**, 18635-18648.

McPhaden, M. J., 2003: Tropical Pacific ocean heat content variations and ENSO persistence barrier. *Geophys. Res. Lett.*, **30**, 1480, doi:10.1029/2003GL016872.

Saha S., S. Nadigam C. Thiaw, J. Wang, W. Wang, Q. Zhang, H. M. van den Dool, H.-L. Pan, S. Moorthi, D. Dehringer, S. Stokes, M. Peña, S. Lord, G. White, W. Ebisuzaki, P. Peng, and P. Xie, 2006: The NCEP Climate Forecast System. *J. Climate*, **19**, 3483-3517.

Torrence, C., and P. J. Webster, 1998: The annual cycle of persistence in the El Niño/Southern Oscillation. *Quart. J. Roy. Meteorol. Soc.*, **124**, 1985-2004.

Wang, B., R. Wu, and R. Lukas, 1999: Roles of the western North Pacific wind variation in thermocline adjustment and ENSO phase transition. *J. Meteor. Soc. Japan*, **77**, 1-16.

Webster, P. J., and S. Yang, 1992: Monsoon and ENSO: Selectively interactive systems. *Quart. J. Roy. Meteorol. Soc.*, **118**, 877-926.

Webster, P. J., 1995: The annual cycle and predictability of the tropical coupled ocean-atmosphere system. *Meteorol. Atmos. Phys.*, **56**, 33-55.

Weisberg, R. H., and C. Wang, 1997: Slow variability in the equatorial west-central Pacific in relation to ENSO. *J. Climate*, **10**, 1998-2017.

Xue, Y., M. A. Cane, S. E. Zebiak, and M. B. Blumenthal, 1994: On the prediction of ENSO: A study with a low-order Markov model. *Tellus*, **46A**, 512-528.

Zebiak, S. E., and M. A. Cane, 1987: A model El Niño-Southern Oscillation. *Mon. Wea. Rev.*, **115**, 2262-2278.